Volume 10, Issue 1, January – 2025 International Journal of Innovative Science and Research Technology
ISSN No:-2456-2165 https://doi.org/10.5281/zenodo.14987767

Mathematical Modeling of Experimental Desorption Curves and Characterization of Thermophysical Parameters of Peulh Cheese Produced in Benin for Solar Drying

Aguemon Wiwegnon Uriel-Longin[1]; Goudjinou Codjo[2];
Tchiekre Michel Henri Daugny[3]; Ahouannou Clément[4]

[1]Université De Kindia, Guinée, Faculté Des Sciences, Département De Mathématiques,
[2]Université d'Abomey-Calavi (UAC), Ecole Polytchnique d'Abomey-Calavi (EPAC), Département de Génie De Technologie Alimentaire, Unité De Recherche En Génie Enzymatique Et Alimentaire (URGEA), 01BP 2009 Cotonou, Bénin
[3]Université Peleforo Gon Coulibaly de Korhogo, Département Mathématiques Physique Chimie, UPR Mathématiques
[4]Université d'Abomey-Calavi (UAC), Ecole polytchnique d'Abomey-Calavi (EPAC), Laboratoire d'Energies et de Mécaniques Appliquées (LEMA), 01BP 2009 Cotonou, Bénin

Publication Date: 2025/03/12

Abstract: The analysis of sorption isotherms is a favored method for gaining insights into the distribution and strength of water bonds, along with their functional availability in biochemical and biological food products. In drying, we are particularly interested in the phenomenon of desorption. This study aims to model desorption isotherms and estimate the thermodynamic parameters of Peulh cheese produced in Benin for solar drying. For this, we experimentally determined the desorption isotherms of the cheese produced at 30°C, 40°C , 50°C and 60°C, by the static gravimetric method, using saturated saline solutions. The desorption curves obtained from the study were compared to theoretical models, including those proposed by Smith, Harking and Jura, Iglesias and Chirife, and the GAB model. Optimization of these theoretical models was performed using the least squares method. Additionally, the net isosteric heat of sorption was calculated via the Clausius-Clapeyron equation. An empirical exponential correlation was established to illustrate the relationship between sorption heat and equilibrium water content. The findings indicated that equilibrium water content decreases with rising temperature across a range of water activity from 5.4% to 97%. The desorption isotherms were classified as type II, characterized by multimolecular adsorption. Notably, the GAB model provided the best fit for the experimentally obtained desorption curves at 50°C. Furthermore, enthalpy-entropy compensation and isokinetic theory were effectively applied to analyze the desorption process of Peulh cheese.

Keywords: *Peulh Cheese, Desorption Isotherms, Mathematical Modeling, Solar Drying, Thermodynamic Properties.*

How to Cite: Aguemon Wiwegnon Uriel-Longin; Goudjinou Codjo; Tchiekre Michel Henri Daugny; Ahouannou Clément (2025). Mathematical Modeling of Experimental Desorption Curves and Characterization of Thermophysical Parameters of Peulh Cheese Produced in Benin for Solar Drying. *International Journal of Innovative Science and Research Technology*, 10(1), 2953-2970. https://doi.org/10.5281/zenodo.14987767

I. INTRODUCTION

Food remains and continues to be the first requirement of man and its quality must be a great concern for researchers in order to guarantee its safety. To satisfy this imperative human necessity, food production must grow exponentially (Swana and al., 2019, Brito and al 2021). Thus, the use of naturally available agricultural, livestock and fishery production remains mandatory (FAO, 2016; MAEP, 2017). Dairy production significantly influences the socio-economic landscape, particularly among pastoral communities. In the Republic of Benin, cow's milk is crucial, contributing over 50% of the annual income for Fulani households (Dossou and al., 2006). However, due to its high water content, milk is susceptible to rapid spoilage caused by microbial growth, especially in warmer climates where cold storage facilities are lacking. This necessitates the adoption of effective preservation techniques tailored to local socio-economic and climatic conditions (Kèkè and al., 2009). One notable dairy product from cow's milk is Wagashi Gassirè, a traditional soft cheese known for its high nutritional value. Produced through the coagulation of fresh whole milk using heat and the enzyme Calotropaine derived from Calotropis procera, Wagashi is widely consumed and holds cultural significance in Benin (Dossou and al., 2016). Locally referred to as Gassiré in Fulfudé, this cheese is a staple source of animal protein for low-income populations and could play a vital role in addressing dietary protein deficiencies (Alalade and al., 2006; Keke and al., 2008). Wagashi production involves various methods, with boiling being the predominant preservation technique. However, challenges such as contamination from improper handling and storage practices persist. A study highlighted that many producers lack adequate facilities to protect against environmental pollutants, leading to potential health risks associated with consumption (Kèkè and al., 2009; Dossou et al., 2016). Despite these challenges, Wagashi remains a key income source for rural women in regions like Borgou and Alibori, where about 70% of the country's cattle are raised (GRET, 2022). In summary, while dairy production, particularly through products like Wagashi Gassirè, offers substantial socio-economic benefits and nutritional support in Benin, addressing preservation challenges and enhancing production practices are critical for ensuring food safety and improving the livelihoods of those involved in this sector. Despite this economic and nutritional importance, the packaging and conservation of cheese present many constraints, such as the ineffectiveness of traditional methods of cheese conservation, resulting in early deterioration of the product in the marketing circuit, the exposure of traditional cheese to the open air; which increases the risks of microbial and chemical contamination, the absence of appropriate packaging for cheese limiting its suitability for conservation, transport and marketing on the local market and for export (Dossou, 2004). Studies of Sessou and al. (2013) showed that the methods of preserving wagashi are limited to frying, traditional smoking, sun drying and daily cooking of the product. For the authors mentioned, sun drying is the predominant preservation method utilized by actresses, with 62.26% of respondents indicating its use, despite significant health risks. While daily cooking can prolong the shelf life of products, it may adversely affect thermolabile nutrients. Nout and al. (2003) highlighted that poor-quality frying oil can compromise the nutritional integrity of food, as saturated fatty acids can lead to triglyceride formation, which is a precursor to lipoproteins and cholesterol in wagashi. Repeated frying of the same product increases the risk of benzopyrene formation, a potential carcinogen. Gomaa and al. (1993) and Kazerouni and al. (2001) noted that traditional smoking methods, while extending shelf life, also pose contamination risks from benzopyrenes and can lead to substantial nutrient losses in wagashi, including fatty acids, tocopherols, and vitamins (Espe and al., 2002). In terms of drying processes, sorption isotherms play a crucial role in understanding the water content throughout drying operations, thereby optimizing these processes. The study of thermophysical parameters is vital for designing food drying and storage equipment, particularly for quantifying isosteric sorption heat necessary for effective moisture removal from products. This article presents both experimental and theoretical sorption isotherms for Peulh cheese produced in Benin at temperatures of 30°C, 40°C, and 50°C, determined via statistical gravimetric methods using saturated saline solutions. The thermodynamic parameters were estimated using the Clausius-Clapeyron equation to assess the energy required for product dehydration.

II. MATHEMATICAL STUDY OF THEORETICAL MODELS OF SORPTION CURVES AND THERMODYNAMIC PARAMETERS

A. *Theoretical Models of Desorption Isotherms*

In this section of our study, we utilize four mathematical equations from existing literature to optimize the experimental curves. These equations are :

➢ *SMITH model*

SMITH model is a linear model. It is often utilized to model the isotherms of agricultural products. Its expression is as follows :

$$X_{eq} = K_1 - K_2 ln(1 - h_r)$$

Where

- K_1 and K_2 are the correlation parameters.
- X_{eq} represents the water content of the product at equilibrium, in % on a dry basis.
- h_r represents the air relative humidity with $h_r < 1$.

$(h_{ri}, X_{eqi})_{1 \le i \le n}$ are a set of n collected data.

We want to determine K_1 and K_2 in a least squares sense. This task consists of minimizing :

$$\sum_{i=1}^{n} \left[X_{eqi} - \left(K_1 - K_2 ln(1 - h_{ri})\right)\right]^2$$

Let us set $f(K_1, K_2) = \sum_{i=1}^{n} \left[X_{eqi} - \left(K_1 - K_2 ln(1 - h_{ri})\right)\right]^2$

Determining K_1 and K_2 in the least squares sense amounts to solving:

$$\begin{cases} \frac{\partial f}{\partial K_1}(K_1, K_2) = 0 \\ \frac{\partial f}{\partial K_2}(K_1, K_2) = 0 \end{cases} \quad (1)$$

$$\frac{\partial f}{\partial K_1}(K_1, K_2) = \sum_{i=1}^{n} (-2) \left[X_{eqi} - \left(K_1 - K_2 ln(1 - h_{ri})\right)\right]$$

$$\frac{\partial f}{\partial K_2}(K_1, K_2) = \sum_{i=1}^{n} 2\, ln(1 - h_{ri})\left[X_{eqi} - \left(K_1 - K_2 ln(1 - h_{ri})\right)\right]$$

We thus obtain the following system :

$$\begin{cases} -nK_1 + \left(\sum_{i=1}^{n} ln\,(1-h_{ri})\right)K_2 = -\sum_{i=1}^{n} X_{eqi} \\ \left(\sum_{i=1}^{n} ln\,(1-h_{ri})\right)K_1 - \left(\sum_{i=1}^{n}\left(ln(1-h_{ri})\right)^2\right)K_2 = \left(\sum_{i=1}^{n} ln\,(1-h_{ri})X_{eqi}\right) \end{cases} \quad (2)$$

We deduce that :

$$K_1 = \frac{\sum_{i=1}^{n} X_{eqi}\,.\sum_{i=1}^{n}\left(ln(1-h_{ri})\right)^2 - \sum_{i=1}^{n} ln\,(1-h_{ri}).\sum_{i=1}^{n} ln\,(1-h_{ri})X_{eqi}}{n\sum_{i=1}^{n}\left(ln(1-h_{ri})\right)^2 - \left(\sum_{i=1}^{n} ln\,(1-h_{ri})\right)^2}$$

$$K_2 = \frac{-n\left(\sum_{i=1}^{n} ln\,(1-h_{ri})X_{eqi}\right) - \left(\sum_{i=1}^{n} ln\,(1-h_{ri})\right).\sum_{i=1}^{n} X_{eqi}}{n\sum_{i=1}^{n}\left(ln(1-h_{ri})\right)^2 - \left(\sum_{i=1}^{n} ln\,(1-h_{ri})\right)^2}$$

Subsequently, we write a Scilab code to calculate K_1 and K_2, knowing h_r and X_{eq}.

- ➢ *IGLESIAS and CHIRIFE Model*

The Iglesias and Chirife model takes the form :

$$X_{eq} = K_1\left(\frac{h_r}{1-h_r}\right) + K_2.$$

Where

- K_1 and K_2 are the correlation parameters.
- X_{eq} represents the water content of the product at equilibrium, in % on a dry basis.
- h_r represents the air relative humidity with $h_r \neq 1$.

$\left(h_{ri}, X_{eqi}\right)_{1\le i\le n}$ are a set of n collected data.

We want to determine K_1 and K_2 in a least squares sense. This task consists of minimizing :

$$\sum_{i=1}^{n}\left[X_{eqi} - K_1\left(\frac{h_{ri}}{1-h_{ri}}\right) - K_2\right]^2$$

$$\text{Let us set} f(K_1, K_2) = \sum_{i=1}^{n}\left[X_{eqi} - K_1\left(\frac{h_{ri}}{1-h_{ri}}\right) - K_2\right]^2$$

Determining K_1 and K_2 in the least squares sense amounts to solving:

$$\begin{cases} \frac{\partial f}{\partial K_1}(K_1, K_2) = 0 \\ \frac{\partial f}{\partial K_2}(K_1, K_2) = 0 \end{cases} \quad (3)$$

$$\frac{\partial f}{\partial K_1}(K_1, K_2) = \sum_{i=1}^{n}\frac{-2h_{ri}}{1-h_{ri}}\left(X_{eqi} - K_1\frac{h_{ri}}{1-h_{ri}} - K_2\right)$$

$$\frac{\partial f}{\partial K_2}(K_1, K_2) = \sum_{i=1}^{n} -2\left(X_{eqi} - K_1\frac{h_{ri}}{1-h_{ri}} - K_2\right)$$

Thus, we thus obtain the following system :

$$\begin{cases} \sum_{i=1}^{n}\left(\frac{h_{ri}}{1-h_{ri}}\right)^2 K_1 + \sum_{i=1}^{n}\left(\frac{h_{ri}}{1-h_{ri}}\right)K_2 = \sum_{i=1}^{n}\frac{h_{ri}X_{eqi}}{1-h_{ri}} \\ \sum_{i=1}^{n}\left(\frac{h_{ri}}{1-h_{ri}}\right)K_1 + nK_2 = \sum_{i=1}^{n} X_{eqi} \end{cases} \quad (3)$$

We infer that :

$$K_1 = \frac{n\sum_{i=1}^{n}\frac{h_{ri}X_{eqi}}{1-h_{ri}} - \left(\sum_{i=1}^{n}X_{eqi}\right)\sum_{i=1}^{n}\left(\frac{h_{ri}}{1-h_{ri}}\right)}{n\sum_{i=1}^{n}\left(\frac{h_{ri}}{1-h_{ri}}\right)^2 - \left[\sum_{i=1}^{n}\left(\frac{h_{ri}}{1-h_{ri}}\right)\right]^2}$$

$$K_2 = \frac{\left(\sum_{i=1}^{n}X_{eqi}\right)\left(\sum_{i=1}^{n}\left(\frac{h_{ri}}{1-h_{ri}}\right)^2\right) - \sum_{i=1}^{n}\left(\frac{h_{ri}}{1-h_{ri}}\right)\left(\sum_{i=1}^{n}\frac{h_{ri}X_{eqi}}{1-h_{ri}}\right)}{n\sum_{i=1}^{n}\left(\frac{h_{ri}}{1-h_{ri}}\right)^2 - \left[\sum_{i=1}^{n}\left(\frac{h_{ri}}{1-h_{ri}}\right)\right]^2}$$

Subsequently, we write a Scilab code to calculate K_1 and K_2, knowing h_r and X_{eq}.

- *HARKING and JURA model*

The Harking and Jura model can be expressed using the following equation :

$$X_{eq} = \sqrt{\frac{K_2}{K_1 - ln(h_r)}} \quad (4)$$

Where

- K_1 and K_2 are the correlation parameters.
- X_{eq} represents the water content of the product at equilibrium, in % on a dry basis.
- h_r represents the relative humidity of the air.

$(h_{ri}, X_{eqi})_{1\le i\le n}$ are a set of n collected data.

The Harking and Jura model is a nonlinear model in $K1$ and K_2. To use the lower squares method to determine K_1 and K_2, it is not easy to proceed as was the case with the Smith model and the Iglesisas chirife model. We will instead use the Levenberg-Marquardt algorithm. The Scilab software provides us with the **lsqrsolve** (Stephen Campbell and al.,2006) command to implement this algorithm.

- *Overview of the Levenberg-Marquardt Algorithm*

Before stating the principle of the Levenberg-Marquardt algorithm, we will give the following definitions :

Définition 1. *Let* $A \in M_n(R)$ *be the set of square matrices of size n.*

if A=$\begin{pmatrix} a_{11} & a_{12}\cdots & a_{1n} \\ \vdots & \vdots\ddots & \vdots \\ a_{n1} & a_{n2}\cdots & a_{nn} \end{pmatrix}$

then diag(A)=$\begin{pmatrix} a_{11} \\ \vdots \\ a_{nn} \end{pmatrix}$

Définition 2. *Let be* $f: (x_1, x_2, \dots, x_n) \in R^n \mapsto f(x_1, x_2, \dots, x_n) \in R$.

The Jacobian matrix of f *is given by :*

$$J = \left(\frac{\partial f}{\partial x_1}\frac{\partial f}{\partial x_2}\frac{\partial f}{\partial x_3}\cdots\frac{\partial f}{\partial x_n}\right)$$

The transpose of J *denoted* J^T *is given by :* $J^T = \begin{pmatrix} \frac{\partial f}{\partial x_1} \\ \frac{\partial f}{\partial x_2} \\ \frac{\partial f}{\partial x_3} \\ \vdots \\ \frac{\partial f}{\partial x_n} \end{pmatrix}$

The Levenberg-Marquardt algorithm (LMA) is employed to address nonlinear least squares problems, as noted by several researchers (K. Madsen and al., 2004; Aude Rondepierre and al., 2018; Henri P. Gavin and al., 2020; Ananth Ranganathan and al., 2004; Marius Kaltenbach, 2022). This algorithm was initially introduced by Kenneth Levenberg in 1944 during his tenure at the Frankford Army Arsenal in the United States. It was later rediscovered by Donald Marquardt in 1963, who was a statistician at the American multinational chemical company DuPont. The primary use of the Levenberg-Marquardt algorithm lies in solving the least-squares curve fitting problem. Given a collection of n empirical pairs (x_i, y_i) representing independent and dependent variables, the goal is to determine the parameters β of the model curve $f(x, \beta)$ such that the sum of the squares of the deviations $S(\beta)$ is minimized (K. Madsen and al., 2004; Aude Rondepierre and al., 2018; Henri P. Gavin and al., 2020; Ananth Ranganathan and al., 2004; Marius Kaltenbach, 2022).

$$S(\beta) = \sum_{i=1}^{n}\left(y_i - f(x_i, \beta)\right).$$

The Levenberg–Marquardt algorithm is an iterative method used for minimization. To initiate this process, the user must supply an initial estimate for the parameter vector β. In scenarios where there is a single minimum, a simple and uninformed choice such as $\beta = (1,1,\dots,1)$ is generally sufficient. During each iteration, the current parameter vector β is updated to a new estimate given by $\beta + \delta$. The adjustment δ is determined by approximating the function $f(x_i, \beta + \delta)$ through its linearization.

$$f(x_i, \beta + \delta) = f(x_i, \beta) + J_i\delta_i$$

Where $J_i = \frac{\partial f(x_i,\beta)}{\partial \beta}$ is the gradient of f, with respect to β.

After calculations, we get :

$$\delta = [(J^T J) + \lambda diag(J^T J)]^{-1} . J^T . \left(y - f(\beta)\right)$$

Where J is the Jacobian matrix, whose i-th row equals J_i and $f(\beta)$ and y are vectors with i-th component $f(x_i, \beta)$ and y_i respectively, λ is a real parameter, J^T is the transpose of the Jacobian matrix, $J^T J$ is a $n \times n$ square matrix. The LMA takes the form :

Where J denotes the Jacobian matrix, where the i-th row is represented as J_i. The vectors $f(\beta)$ and

y have their $i - th$ components defined as $f(x_i, \beta)$ and y_i respectively. Additionally, λ is a

Real parameter. The transpose of the Jacobian matrix is denoted as J^T, and the product $J^T J$ results in an

$n \times n$ square matrix. The Levenberg-Marquardt Algorithm (LMA) is formulated as follows :

- β_0 is the initial value.
- $\beta_n = [J^T J + \lambda diag(J^T J)]^{-1} . J^T . \left(y - f(\beta)\right)$.
- $\beta_0 = \beta_0 + \beta_n$ update (Samir KENOUCHE, 2018)
- Stop criterion

➢ *GAB model*

The Guggenheim-Anderson-de Boer (GAB) model, established in 1981, serves as a systematic extension of the Brunauer-Emmett-Teller (BET) theory. This model is grounded in the premise of multilayer physical sorption without lateral interactions among adsorbate molecules. The GAB model has demonstrated strong correlations in moisture sorption isotherms up to a water activity level of approximately 0.9, as noted by Goudjinou and al. (2017).

➢ *Key Features of the GAB Model :*

- Estimation of Water Binding: The GAB model effectively estimates the quantity of water bound to primary adsorption sites, denoted as X_m.
- Physical Parameters: It incorporates parameters that provide a physical interpretation of the sorption process, allowing for a deeper understanding of how temperature influences sorption curves through Arrhenius-type equations.
- Mathematical Representation: The GAB model is mathematically expressed to encapsulate these phenomena, although specific equations were not detailed in the provided sources.

In summary, the GAB model enhances our understanding of moisture sorption dynamics by integrating theoretical frameworks with empirical observations, making it a valuable tool in fields such as food science and materials engineering.

$$X_{eq} = \frac{K_1 K_2 K_3 h_r}{(1 - K_3 h_r)(1 - K_3 h_r + K_2 K_3 h_r)} \qquad (5)$$

In contrast to the Harking and Jura model, which incorporates two variability parameters, the GAB model features three variability parameters K_1, K_2 and K_3. These parameters are defined as follows :

- X_{eq} : It represents the moisture content of the product.
- K_1 : This parameter indicates the water content that corresponds to the full occupancy of all sorption sites in the monomolecular layer of water within the product, expressed as a percentage relative to the dry matter.
- K_2 : This is the GAB constant.
- K_3 : It serves as a corrective factor for the properties of the multilayer (Ferradji and al.,2008)

We also use the Levenberg-Marquardt algorithm to calculate K_1, K_2 and K_3 because the GAB model is a nonlinear model in K_1, K_2 and K_3.

The best model is retained on the values of the squared error, error L^2.

B. Determining the Thermodynamic Properties of the Desorption Process.

➢ *Energy of Activation*

The Arrhenius equation describes the relationship between the monolayer water content (X_m) in the GAB model and temperature. Specifically, it indicates how temperature influences the equilibrium moisture content by affecting the rate of water adsorption and desorption processes. According to Goudjinou and al. (2017), this correlation is critical for understanding moisture sorption phenomena in various materials, including food products.

$$X_m = X'_m exp\left(\frac{-E_a}{RT}\right) = X'_m exp\left(\frac{-E_a}{R}\frac{1}{T}\right) \qquad (6)$$

With Ea: the energy of activation (J/mol), X'm: the collision frequency (%MS).

The graph representation ln (Xm) = f(1/T), permits to determine the slope

Ea/R and the ordinate at the origin $ln(X'm)$.

➢ *The Desorption's net Isosteric Heat*

The Clausius-Clapeyron equation, grounded in solid theoretical principles, is commonly employed to calculate the total heat of sorption (Qst) in agricultural products (Iglesias and Chirife, 1976; Kiranoudis and al., 1993). It serves to estimate the heat necessary for the evaporation of both free and bound water within a product. The equation can be expressed as follows :

$$\frac{d}{dT}\left(ln(P)\right) = \frac{Q_{st}}{R_0 T^2} \qquad (7)$$

For pure water in its natural state, the equation 8 can be simplified to :

$$\frac{d}{dT}\left(ln(P_0)\right) = \frac{L_v}{R_0 T^2} \qquad (8)$$

- With P : The water vapor pressure of the product at the given temperature.
- Po : The saturation water vapor pressure at temperature T.
- Lv : The latent heat of vaporization of pure water in its free state.

- *We Obtain after Calculations :*

$$\frac{d}{dT}\left(ln\left(\frac{P}{P_0}\right)\right) = \frac{dln(a_W)}{dT} = \frac{q_{st}}{R_0 T^2} \tag{9}$$

The net isoteric heat of sorption, denoted as q_{st}, is defined by equation : $q_{st} = Q_{st} - L_v$.

This value (in kJ/mol) corresponds to the equilibrium wate content, X_{eq}.

The relationship can be expressed through the following equation :

$$ln(a_\omega) = \left(\frac{-q_{st}}{R_0}\right)\frac{1}{T} + C_{st} \tag{10}$$

By graphically representing equation [eq1] for a fixed water content and a known value of R_0, we can determine both the slope $\frac{-q_{st}}{R_0}$ and the integration constant C_{st}. Using the slope obtained for each equilibrium water content X_{eq}, we can calculate the corresponding net isoteric heat. This enables us to plot the curve $q_{st} = f(X_{eq})$. In addition, Tsami and al. (1990) proposed an empirical correlation to characterize the relationship between the net isosteric heat of desorption and the equilibrium water content, given by :

$$q_{st} = q_0 exp\left(\frac{-X_{eq}}{X_0}\right) \tag{11}$$

In this equation, q_o represents the net isosteric heat of desorption for the initial water molecules in the product (measured in kJ/mol), while X_o indicates the characteristic water content at which this heat is determined, specifically at 63% (Kiranoudis and al., 1993).

➢ *Overview of Enthalpy-Entropy Compensation Theory.*

The differential entropy is determined using the Gibbs-Helmholtz equation (13), with the Gibbs free energy derived from equation (14).(Giraldo and al, 2011; Goudjinou and al, 2017) :

$$\Delta S = \frac{-q_{st} - \Delta G}{T} \tag{12}$$

$$\Delta G = RT_0 ln\left(\frac{P}{P_0}\right) = RTln(a_\omega) \tag{13}$$

$$ln(a_\omega) = \frac{-q_{st}}{RT} + \frac{\Delta S}{R} \tag{14}$$

Using the y-intercept of the isostere lines for each equilibrium water content X_{eq}, the corresponding differential entropy of sorption is determined, and the curve $\Delta S = f(X_{eq})$ is plotted.

In accordance with compensation theory, the linear relationship between enthalpy and entropy for a given reaction is expressed as :

$$q_{st} = T_\beta(\Delta S) + \Delta G_\beta \tag{15}$$

Here, T_β represents the isokinetic temperature at which all reactions in the series proceed at the same rate, and ΔG_β denotes the free energy at that temperature, used to determine whether the water sorption process is spontaneous $(-\Delta G_\beta)$ or non-spontaneous $(+\Delta G_\beta)$. Both T_β and ΔG_β are derived from the plot of the curve $q_{st} = f(\Delta S)$.

➢ *Compensation Theory Test*

Krug and al. (1976) and Madamba and al. (1996) propose a method for testing the compensation theory by comparing the isokinetic temperature to the harmonic mean temperature, denoted as (Th_m). This harmonic mean temperature is defined in the context of thermodynamic relationships, as elaborated by Goula and al. (2008) and Giraldo and al. (2011).

$$Th_m = \frac{n}{\sum_{i=1}^{n}\left(\frac{1}{Tn}\right)} \tag{16}$$

Isokinetic temperature (T_β) is calculated by linear regression for all data sets with a 95% confidence interval.

$$T_\beta = \frac{\sum(q_{st} - \overline{q_{st}})(\Delta S - \overline{\Delta S})}{(\Delta S - \overline{\Delta S})^2} \tag{17}$$

$$Var(T_\beta) = \frac{\sum(q_{st} - \overline{\Delta G_\beta} - T_\beta \Delta S)^2}{(m-2)\sum(\Delta S - \overline{\Delta S})^2} \tag{18}$$

With n : total number of isothermal points; m : number of $(q_{st}, \Delta S)$ data pairs; $(\overline{q_{st}})$: the average enthalpy and $\overline{\Delta S}$: the average entropy.

III. MATERIAL AND METHODS

The material used consists of fresh milk from daily milking cows purchased from the farm of the Faculty of Science and Technology (FSA) of the University of Abomey-Calavi. The samples of fresh leaves of Calotropis procera were collected on the Campus of the University of Abomey-Calavi then washed and stored at -5°C in the laboratory for different uses.

➢ *Preparation of Coagulant Extracts*

For the preparation of the coagulant, the leaves of Calotropis procera were harvested, washed, weighed, then pounded in a clean mortar. The crushed material obtained was mixed with a small amount of fresh milk. The mixture obtained was filtered using a sieve then added directly to the milk over the heat.

- *Preparation of Peulh Cheese*

Figure 1 shows the different stages of Peulh cheese production. The modified method of Dossou and al. (2016) was used for product development. After preheating the milk over a low heat at 60°C for 5 to 10 minutes, the coagulant was added then heated to a temperature of 95°C until the formation of curds supernatant the whey. The quantities of calotropis procera leaves used varied between 35 and 40 g per liter of milk. The appearance of the cream on the surface in the form of an oily foam characterizes coagulation. At this stage, the fire is activated for 2 to 3 minutes in order to have a temperature of 100°C. After coagulation, the curds were poured with a ladle into strainers to drain, just after cooling. The cheese loaf thus obtained in each strainer is a very hydrated soft paste, which oozes for 1.5 to 2 hours. Finally, the cheese was stored in the refrigerator at +4°C.

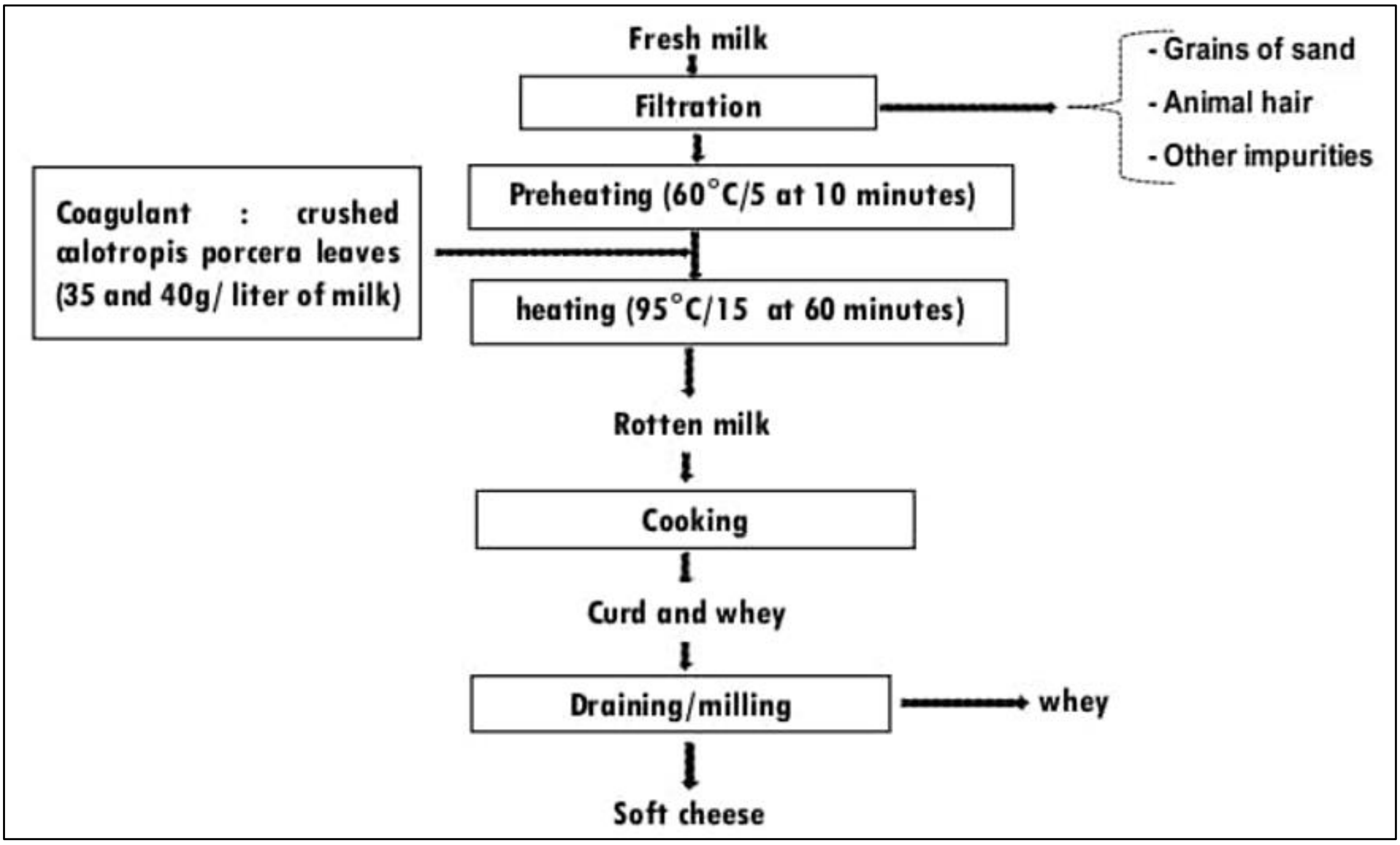

Fig 1 Technological Diagram of the Production of Peulh Cheese (Wagashi)

- *Determination of Desorption Isotherms of the Cheese Produced*

The static gravimetric experimental method is a widely used technique for determining the desorption isotherms of various food products, including peulh cheese. This method involves the use of saturated salt solutions to create controlled relative humidity environments within airtight jars. The method employs several salts such as $LiBr$, $K0H$, $LiCl$, $MgCl2$, $C0Cl2$, Kl, $NaCl$, KCl and K_2S0_4 to prepare saturated solutions. Each salt is dissolved in a specific mass M_i of distilled water in a jar of volume V. The mixture is stirred until saturation is achieved, resulting in a solution that maintains a constant relative humidity within the jar. The jars containing the saturated solutions are placed in a ventilated, temperature-controlled oven. This setup allows for the generation of relative humidities ranging from 5.4% to 97% at fixed temperatures of 30°C, 40°C, 50°C, and 60°C. The static gravimetric method measures the weight change of the peulh cheese samples over time until equilibrium is reached with the water vapor pressure in the jar. This process can be time-consuming due to the slow diffusion rates of water vapor. This method is crucial for understanding moisture sorption and desorption characteristics in food products, which directly affect their shelf life, stability, and quality. By determining desorption isotherms, researchers can better predict how peulh cheese will behave under various storage conditions, thus informing packaging and preservation strategies. In summary, the static gravimetric method using saturated salt solutions provides an effective means to evaluate the moisture dynamics of peulh cheese, contributing valuable data for food science and technology.

Table 1 Saturated Salt Solutions; Variation of Saturations.

Variables	**LiBr**	**KOH**	**LiCI**	**MgCl2**	**CoCl2**	**KI**	**NaCl**	**KCl**	**K2SO4**
Masses Mi de sel (g)	120	300	120	120	120	264	264	120	250
Volumes V d’eau (ml)	160	200	150	200	200	200	200	200	1500
Solubilités (g/l) à 25°C	789	1100	769	542	542	1430	358	344	350

The masses obtained are distinct for the different types of salts used in the saline solutions. This difference in the masses of the salts is due to the difference in solubilities. The desorption experiment consisted of placing a portion of the cheese sample to be desorbed in hermetically sealed isothermal jars, which respectively contained the saturated solutions of salts mentioned above, set at a constant relative humidity (Table 2) due to the nature of the salt and at a constant temperature set in the oven. The desorption tests were carried out at 40, 50 and 60°C. Before introducing the samples into the isothermal jars, they were placed in the oven for 24 hours to ensure the adaptation of the saline solutions to the required set temperatures. The isothermal jar and sample assembly was weighed every 24 hours until the mass stabilized. When the different equilibrium masses (Meq) are obtained for different imposed conditions, the tested products are immediately oven-dried at 105°C ±2°C to determine their anhydrous mass (Ms). From the anhydrous mass (Ms) obtained, the water content of the product on a dry basis is determined by the following equation :

$$X_{eq} = \frac{M_{eq} - M_s}{M_s} \tag{19}$$

The values of the couples (H_{ri}, X_{eqi}) with $i \in \{1, \dots, n\}$, allowed us to experimentally plot the sorption curves of the cheese. Thus, the water content of the cheese at equilibrium is determined as follows :

$$X_{eq} = f(a_w)T_s \tag{20}$$

T_s : System equilibrium temperature in Kelvin; a_w : water activity of the product, in decimal fraction given by the relation :

$$a_w = \frac{P_V}{P_{vsat}} = \frac{H_r(\%)}{100} \tag{21}$$

Table 2 gives the standard values of water activity depending on the salts and the experimental temperature.

Table 2 Standard Water Activity values as a Function of Salt type and Temperature.

Salts	$ln(aw) = \frac{K_1}{T} - K_2$		**aw (%)**		
		30°C	**40°C**	**50 °C**	**60 °C**
LiBr	Ln aw = (620.6358 x 1/T) - 4.8327	6.20	6.00	5.70	5.40
KOH	Ln aw = (2094.4890 x 1/T) - 9.4977	7.20	6.70	5.90	5.60
LiCl	Ln aw = (10.8233 x 1/T) - 2.2193	11.30	11.3	11.20	11.00
MgCl2	Ln aw = (151.0652 x 1/T) - 1.6271	32.40	32.10	31.10	29.9
CoCl2	Ln aw = (982.7329 x 1/T) - 5.0477	61.8	58.60	52.60	48.00
KI	Ln aw = (258.1545 x 1/T) - 1.2388	67.89	66.96	65.26	63.78
NaCl	Ln aw = (23.1092 x 1/T) - 0.3607	75.1	74.90	74.50	74.40
KCl	Ln aw = (157.0587 x 1/T) - 0.6967	83.6	83.00	81.70	80.7
K2SO4	Ln aw = (52.7544 x 1/T) - 0.2046	97.00	96.70	96.10	96.00

Source : Labuza and al. (1985) ; (Goudjinou, 2018) .

The mathematical formulas used for simulating experimental desorption isotherms in cheese production include those developed by Smith, Iglesias and Chirife, Harking and Jura, and the GAB model. Understanding these isotherms is crucial for determining the optimal conditions of temperature and humidity necessary for cheese preservation.

As a result, the various thermodynamic parameters identified previously are derived directly or indirectly from the equilibrium conditions indicated by the experimental curves. These parameters are essential for optimizing drying processes. The isotherms enable the quantification of the isosteric heat of sorption during the drying of the product, effectively facilitating the transition of the product from its fresh state to a dehydrated state that enhances its preservation.

IV. RESULTS AND DISCUSSION

Obtaining experimental desorption curves is a time-consuming process, as these curves are derived from multiple isothermal points (H_{ri}, X_{eqi}) where $i \in \{1, \dots, n\}$. These points are determined under specified conditions across various temperatures and humidity levels. For products with high water content, the initial isothermal point typically requires an average of 7 to 10 days to establish (Ahouannou and al., 2023). The duration is influenced by both the mass of the sample and the imposed isothermal conditions. This finding aligns with previous observations by Ahouannou and al. (2010) regarding the isotherms of ginger, red pepper, and cassava. While this method is effective, it can be quite tedious and is susceptible to significant errors if the operator lacks expertise (Swana and al., 2019). Table 3 presents pairs of parameters (aw, Xeq) that are representative of the isothermal points.

Table 3 Equilibrium Water Content (X_{eq} in g Water/100g ms) as a Function of aw (%) at 30, 40, 50 and 60 °C.

Salts	**T= 30°C**		**T= 40°C**		**T= 50 °C**		**T= 60 °C**	
	a_w	Xeq	a_w	Xeq	a_w	Xeq	a_w	Xeq
LiBr	6.20	4.45	6.00	3.35	5.70	3.11	5.40	3.01
KOH	7.20	5.11	6.70	4 .46	5.90	3.98	5.60	3.41

LiCl	11.30	6.37	11.3	5.85	11.20	5.02	11.00	4.25
MgCl2	32.40	10.20	32.10	7.59	31.10	7.23	29.9	6.19
CoCl2	61.8	16.20	58.60	13.01	52.60	11.03	48.00	9.01
KI	67.89	17.88	66.96	16.03	65.26	14.29	63.78	11.39
NaCl	75.1	21.94	74.90	20.99	74.50	17.60	74.40	14.49
KCl	83.6	27.53	83.00	25.42	81.70	21.03	80.7	16.82
K2SO4	97.00	39.25	96.70	35.87	96.10	29.86	96.00	25.87

Source : Labuza and al. (1985) ; (Goudjinou, 2018)

The data presented in this table indicate that, for a consistent saturated saline solution, an increase in temperature within the controlled environment leads to a reduction in both the ambient relative humidity and the equilibrium water content of the product. This phenomenon is primarily due to the heightened excitation of water molecules at higher temperatures, which diminishes intermolecular attraction forces (Goudjinou and al., 2017). Our results are consistent with the isotherms observed in many agri-food products (Ahouannou and al., 2010; Benseddik and al., 2018; Goudjinou and al., 2017). However, some researchers (Al-Muhtaseb and al., 2004; Gabas and al., 1999) have identified an inversion effect in sugar-rich products, such as fruits. In these cases, the isotherm curves intersect at higher water activity levels (above 0.6). This effect arises from the increased solubility of sugars at elevated temperatures, which subsequently reduces water mobility. The relationship between equilibrium water content and temperature is critical, as it significantly influences the chemical and microbiological reactions that contribute to product deterioration.

- *Mathematical models' validation*

The experimental results were assessed in relation to various theoretical models, specifically those developed by Smith, Iglesias, Chirife, Harkins, Jura, and the GAB model. The evaluation of the Smith and Iglesias models utilized the linear least squares method, while the fitting of the Harkins and Jura and GAB models was conducted using the Levenberg-Marquardt algorithm. This algorithm was executed through the lsqrsolve command in Scilab, which facilitated the determination of model parameters. The resulting parameters, along with their corresponding squared errors L^2 from the fits, are compiled in tables.

Table 4 Estimated values of Adjustment Parameters and Statistical Criteria for model Choice.

T (°C)	**Parameters**	**Smith**	**Iglesias and Chirife**	**Harking and Jura**	**GAB**
30	K1	0.0466438	0.0110094	0.0603943	0.0913001
	K2	0.1109593	0.103129	0.0150283	17.345735
	K3	-	-	-	0.7993217
	L^2	0.0052408	0.0453498	0.0186977	0.0089076
40	K1	0.0377005	0.0123685	0.0524226	0.0860387
	K2	0.1086282	0.0883597	0.0124476	13.162767
	K3	-	-	-	0.8001385
	L^2	0.0043496	0.0380353	0.0246636	0.0252542
50	K1	0.034306	0.0122765	0.0542399	0.0749813
	K2	0.0938553	0.0747307	0.0094464	15.695677
	K3	-	-	-	0.7929779
	L^2	0.0028191	0.0245879	0.0092841	0.0031229
60	K1	0.0255492	0.0170727	0.0206028	0.0581368
	K2	0.090093	0.0553875	0.0063413	22.293994
	K3	-	-	-	0.8368504
	L^2	0.008912	0.0111382	0.0932307	0.014994

The examination of the table indicates that the adjustment constants (K1, K2, K3) and the L^2 error values fluctuate based on the model used and the temperature conditions. The models exhibiting the lowest L^2 error values signify an excellent fit to the experimental data. Among these, the model with the minimum L^2 error was deemed the most suitable for representing the cheese desorption isotherms. Among all models analyzed, the Smith model demonstrated the lowest error values, establishing it as the most effective model for fitting the cheese desorption isotherm data across the entire temperature spectrum studied, which ranges from 30°C to 60°C. Additionally, it is noteworthy that the GAB model also achieved relatively low L^2 values. All four models evaluated reached their lowest L^2 values at a temperature of 50°C. According to Medeiros and al. (2006), the parameter K_3 in the GAB equation plays a crucial role in defining sorption isotherms. Specifically, when $K_3 \leq 10$, the isotherm is categorized as type III; conversely, if $K_3 \geq 10$, it falls into type II. In this study, the K_3 values derived from the GAB model varied between 79.29779 and 83.68504, indicating that the desorption isotherms are classified as type II. The sigmoidal shape observed here is indicative of multimolecular adsorption and illustrates the progressive thickening of the adsorbed layer. This type of isotherm is commonly associated with the hygroscopic properties of various agri-food products

(Goudjinou and al., 2017; Bidias and al., 2022; Ahouannou and al., 2023). The theoretical curves generated from the four models examined are displayed in Figures 2, 3, 4, and 5.

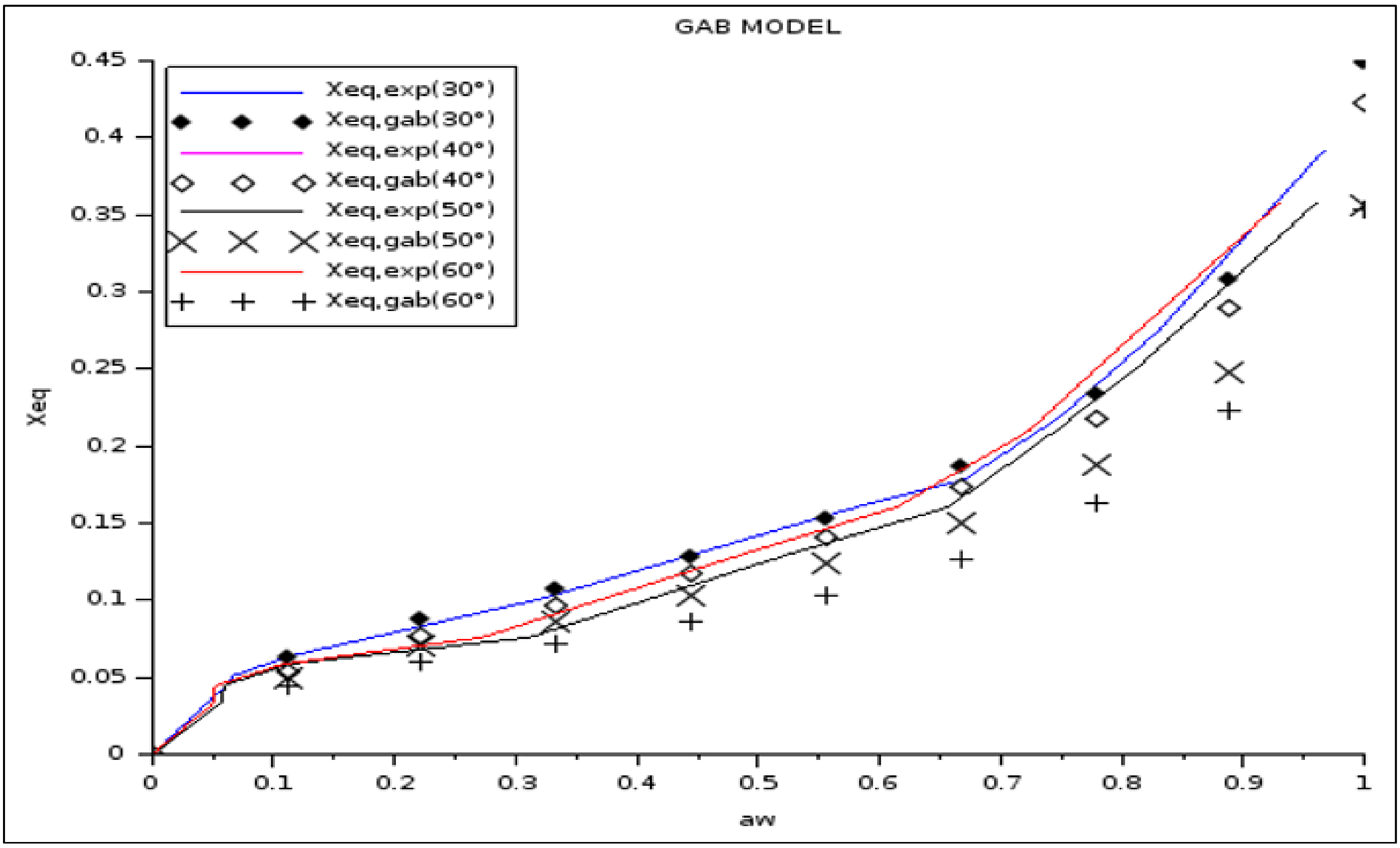

Fig 2 Experimental and theoretical curves at 30, 40, 50 and 60 °C for GAB model

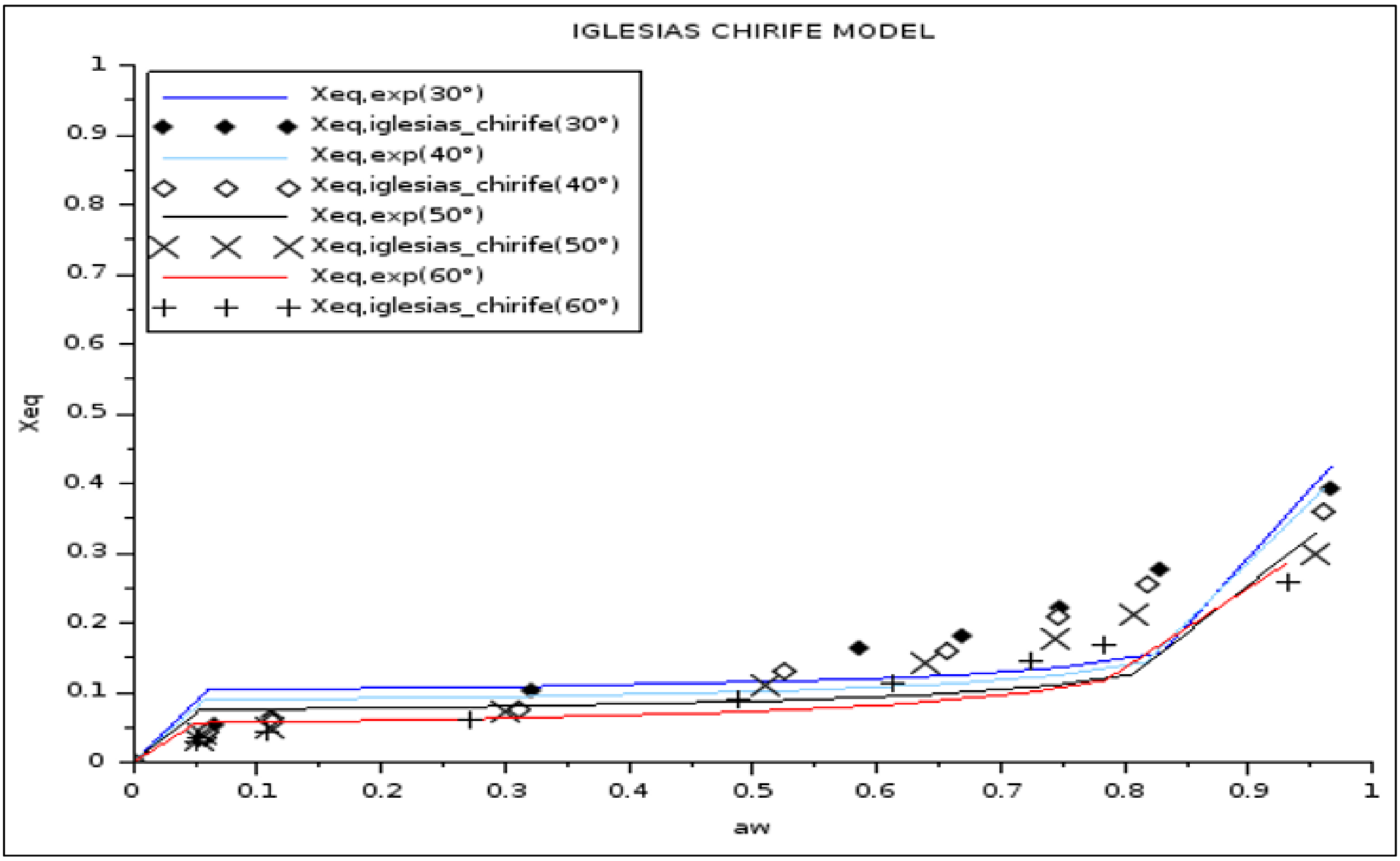

Fig 3 Experimental and theoretical curves at 30, 40, 50 and 60 °C for Iglesias Chirife model

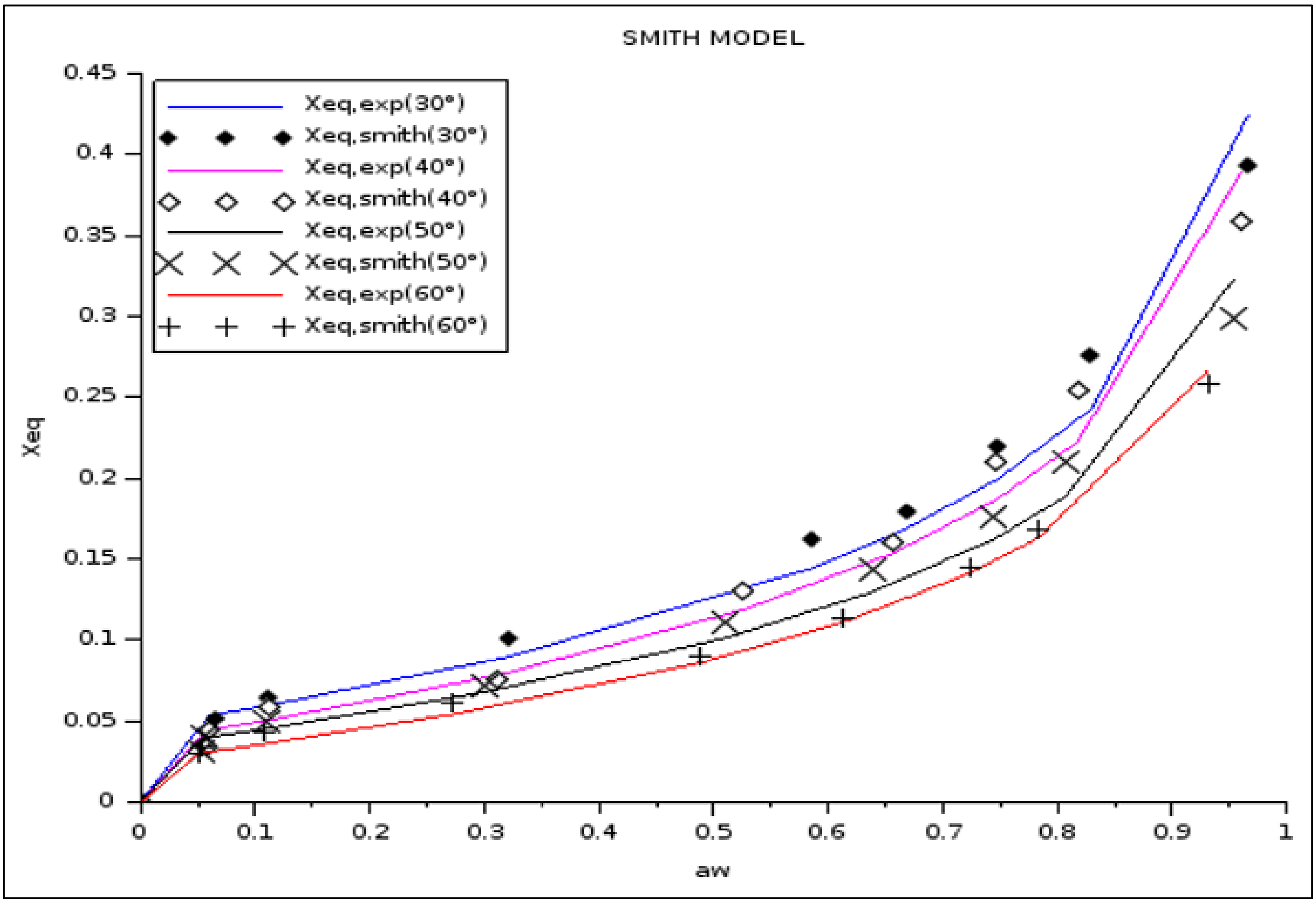

Fig 4 Experimental and theoretical curves at 30, 40, 50 and 60 °C for Smith model

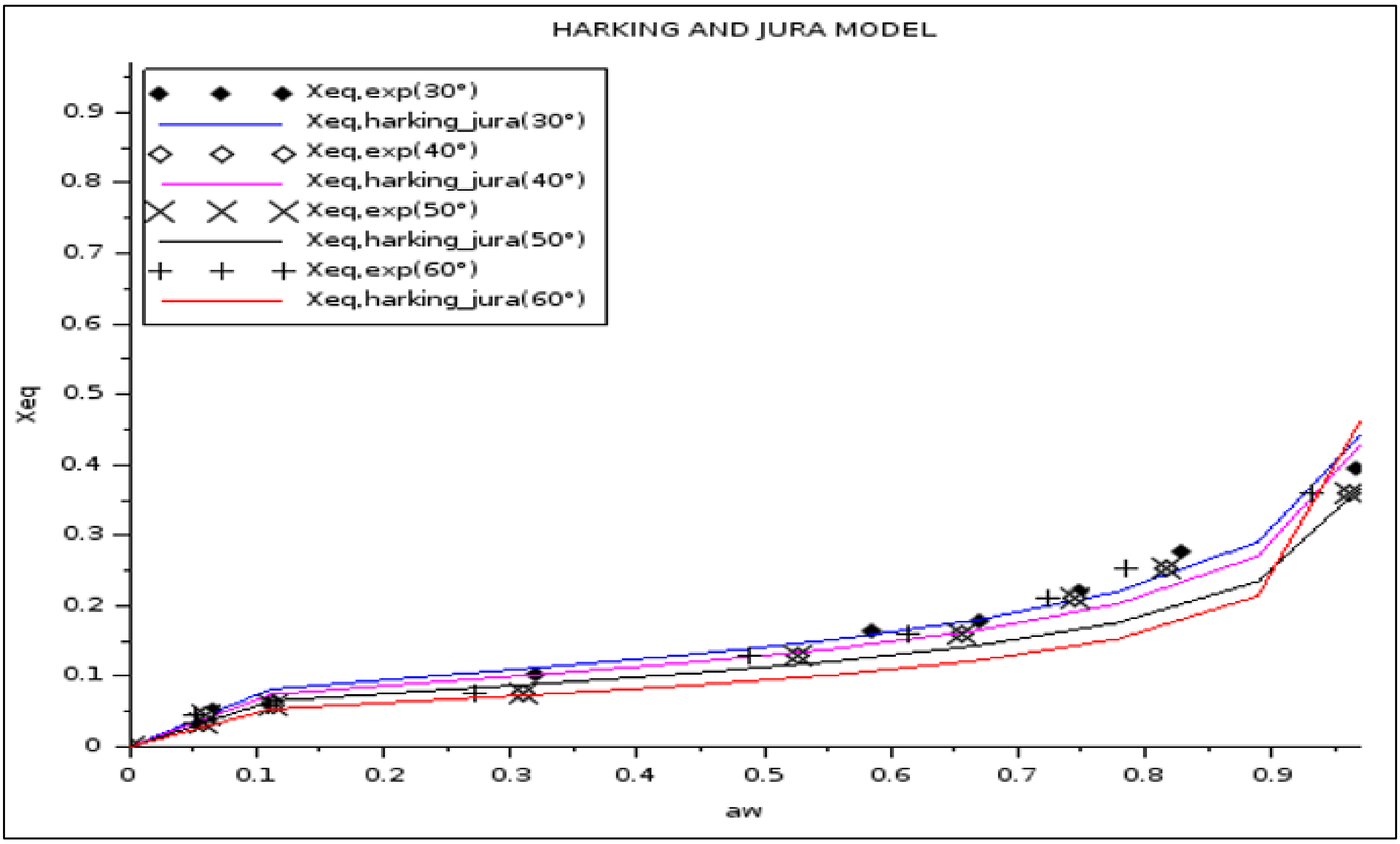

Fig 5 Experimental and theoretical curves at 30, 40, 50 and 60 °C for Harking Jura model

Figure 6 illustrates the residual error curves obtained from comparing the experimental data with the theoretical models of Smith, Iglesias and Chirife, Harkins and Jura, and GAB at 50°C.

An examination of this figure indicates that the residual Smith and GAB curves closely align with the abscissa axis within the water activity range of 5.5% to 97%. This alignment underscores the efficacy of these models at a temperature of 50°C. Consequently, this observation provides a clear rationale for the lower values observed for Smith's L^2 (0.0028191) and GAB (0.0031229) at 50°C.

- *Isosteric Heat of Sorption*

The net isosteric heat of sorption is obtained from the slope of the curve derived using Equation (22) for a specific equilibrium water content, as illustrated in Figure 4. To facilitate this, water activity values at different temperatures are computed for each equilibrium water content by utilizing the GAB model parameters in their transformed format, as outlined by Maroulis and al. (1995), leading to Equation (35). By analyzing the slopes of the isosteres, the corresponding net isosteric heat can be calculated for each equilibrium water content X_{eq}, enabling the construction of the curve $qst = f\left(X_{eq}\right)$ (see Figure 4). The experimental results for net isosteric heat and differential entropy exhibited a strong correlation, achieving an R^2 value of 1.

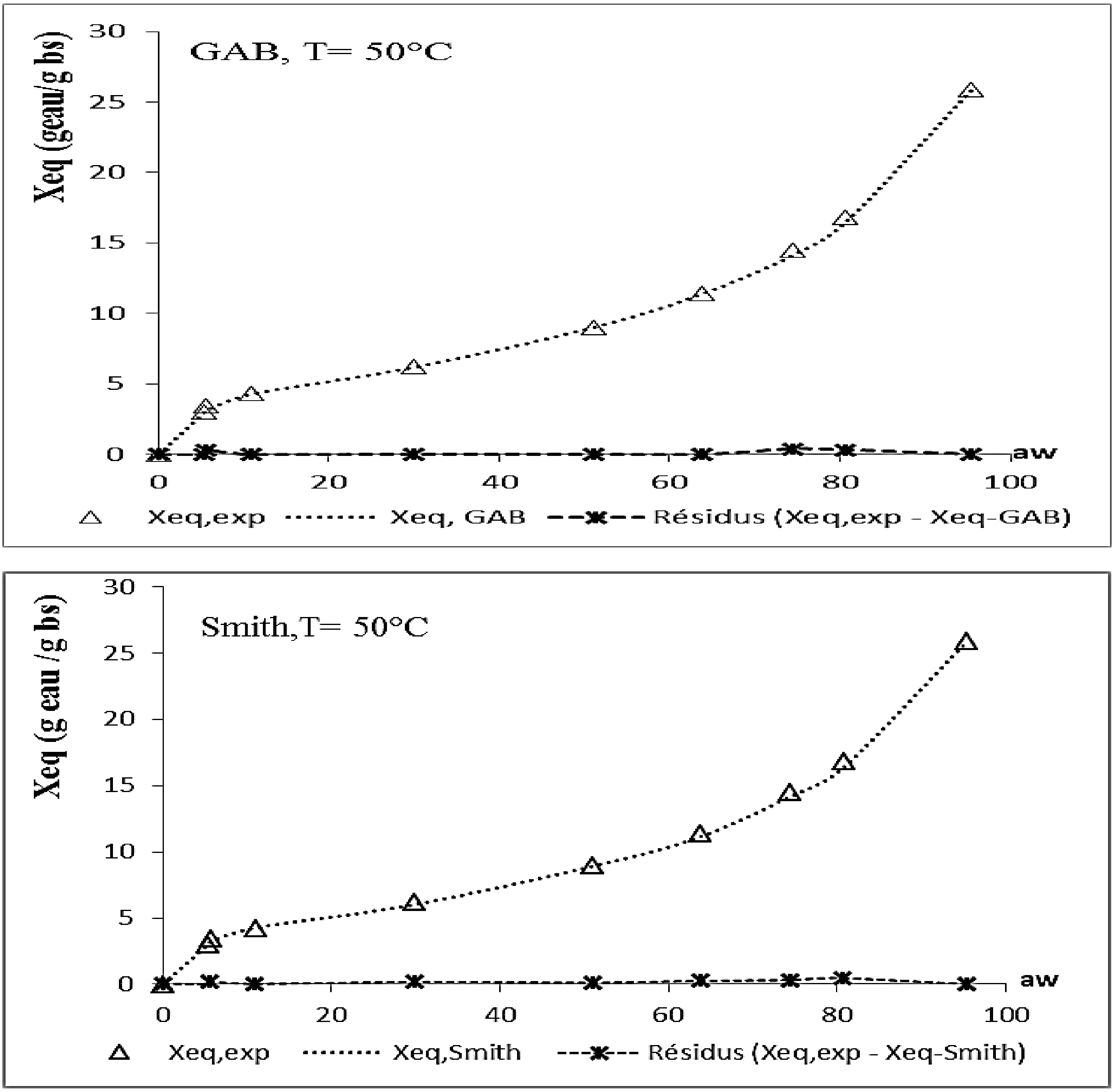

Fig 6 Residual error curves between experimental isotherms and predicted by GAB and Smith, at 50°C.

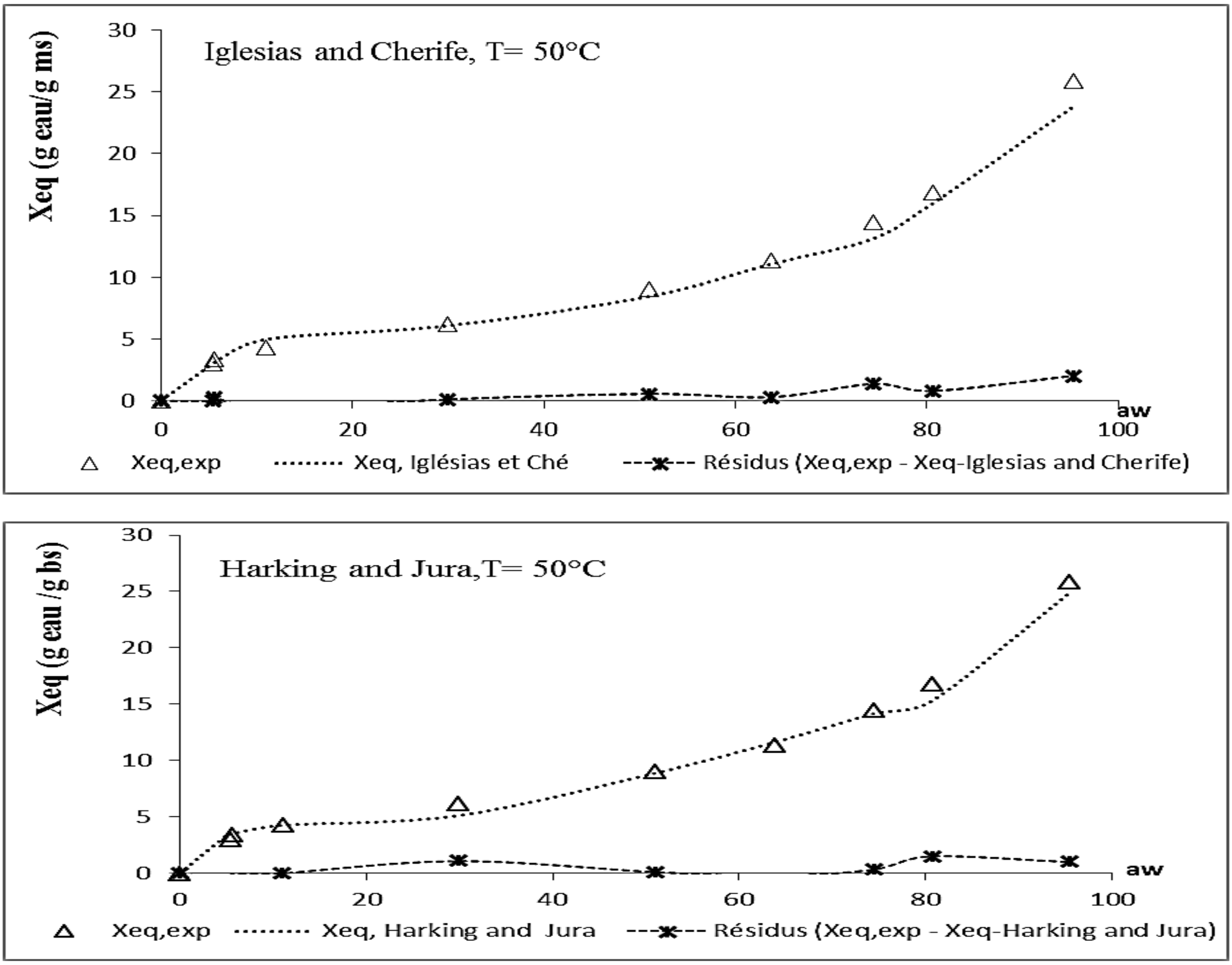

Fig 7 Residual error curves between experimental isotherms and predicted by Harking and Jura, Iglesias and Chirife at 50°C.

$$a_w = \left[2 + \left(\frac{X_m}{X_{eq}} - 1\right)C - \left\{\left(2 + \left(\frac{X_m}{X_{eq}} - 1\right)C\right)^2 - 4(1-C)\right\}^{\frac{1}{2}}\right] \Big/ [2K(1-C)] \tag{22}$$

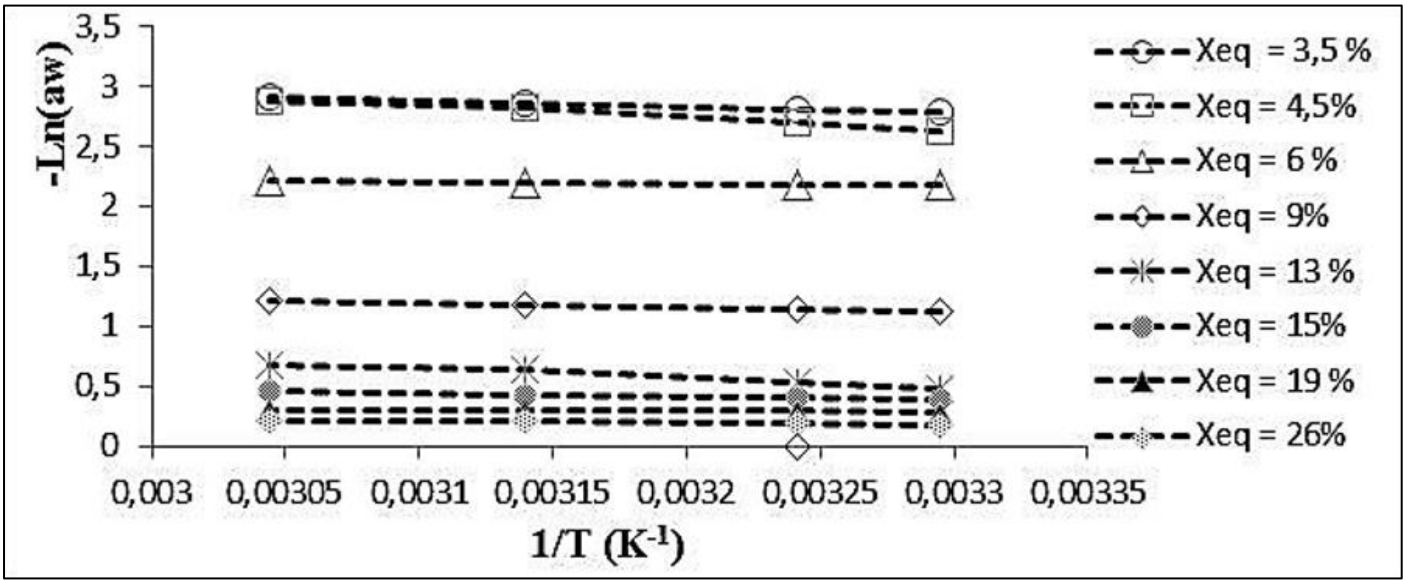

Fig 8 The desorption isoteres of Peulh cheese for certain values of Xeq

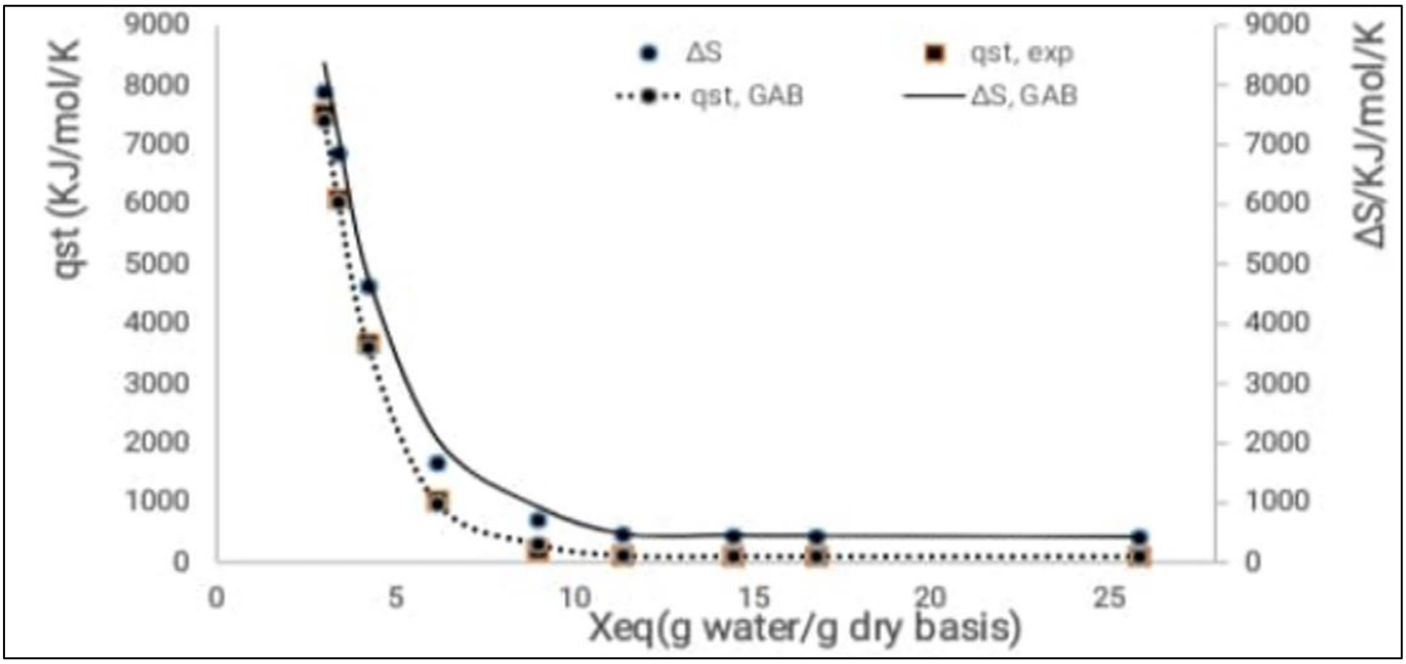

Fig 9 Isosteric heat and experimental differential entropy and predicted by GAB

Figure 8 illustrates that at elevated water contents, both the net isosteric heat and the differential entropy of desorption converge towards zero. This suggests that the isosteric heat of sorption aligns with the heat of water condensation. Within this high water content range, the net isosteric heat remains positive, indicating an endothermic interaction between water and the product substrate, which is associated with the dissolution of sugars. In contrast, at lower water contents, the initial heat of sorption is markedly high, reflecting the strong interactions between the components of the agricultural product and water. As water content rises, the availability of sorption sites diminishes, resulting in a decrease in heat of sorption values. At high humidity levels, the isosteric heat of desorption (qst) becomes minimal in comparison to the latent heat. This behavior can be explained by the presence of highly active polar sites in tomatoes. When these sites are covered by water molecules forming a monolayer, further interactions are significantly reduced (Tasmi and al., 1990).

Additionally, other studies (Boki and al., 1990; Salgado, 1994) suggest that in a narrow humidity range, the swelling of certain products due to increased water content can expose new strong adsorption sites, temporarily raising the isosteric heat.

The specific water content of the product, at which the net isosteric heat of desorption was calculated, is 63%(X_0). Additionally, the net isosteric heat of desorption for the initial water molecules (q_0) was obtained using the linear empirical Equation (22) through the least squares method. These findings are presented in Table 5.

Table 5 Values of Xo and qo of Peulh cheese

Parameters	**T= 30°C**	**T= 40°C**	**T= 50°C**	**T= 60°C**
X_o(g water/gms)	0,08075639	0,07649098	0,06249227	0,05261513
q_o(KJ/mol)	16,4329266	16,3095454	16,3956327	16,378185
r^2	0,965724	0,934134	0,98546	0,99999

Analysis of the data in this table reveals that an increase in temperature results in a decrease in the characteristic water content (X0=0.0808 g of water/g dry matter). Meanwhile, the net heat of isosteric desorption for the first layers of water molecules in the product (q0) remains nearly constant at 16.37±0.9816.37±0.98 kJ/mol across the studied temperature range.

These findings align closely with the 16.9916.99 kJ/mol reported by Benseddik et al. (2014) for the desorption of fig fruit. The q0 parameter is particularly significant, as it provides valuable insight into the physicochemical interactions between water and the product's major constituents, as well as the water's state within the product. This information is crucial for estimating energy requirements during the drying process (Kiranoudis et al., 1993).

- *Enthalpy-Entropy Compensation*

The Enthalpy-Entropy compensation theory is extensively utilized to assess the physical and chemical phenomena associated with sorption reactions (Goudjinou and al., 2017). This theory elucidates the inherent variations in the interactions between the solvent and the substrate, and it highlights a perfect linear correlation between these two state functions (Benhamou and al., 2010). The data presented in Figure 9 illustrate a perfect correlation, with $(R^2 = 1)$, between the enthalpy and entropy parameters.

The calculated isokinetic temperature T_β and harmonic mean temperature Thm are $314.171K$ and 314.459, respectively, while the free energy change ΔG_β is measured at $308.18 J/mol$. When comparing these values, the isokinetic temperature for Peulh cheese is notably lower than those reported for garlic $(348K)$ (Madamba and al., 1996), mango $(463 \pm 4K)$ (Gabas and al., 2007), and spaste $(330.7K)$ (Shittu and al., 2015). In contrast, Kakou and al. (2015) reported an exceptionally low T_β value of $0.0034K$ for cocoa beans. The harmonic mean temperature $Thm = 314.459K$ reinforces the applicability of isokinetic theory to the desorption of water from Peuhl cheese.The relationship between T_β and Thm indicates that the enthalpic process is predominantly driven; according to Leffler (1995), when $Thm < T_\beta$, it suggests that the enthalpic component is the driving force. Conversely, if $Thm < T_\beta$, the process would be classified as entropically controlled. The positive value of free energy ΔG_β $(308.18 J/mol)$ indicates that the desorption process is non-spontaneous (Benhamou and al., 2010). This observation aligns with the thermodynamic principles underlying the Enthalpy-Entropy compensation process, which reflects the structuring and destructuring dynamics of water. The changes in enthalpy represent energy fluctuations between water molecules and the surrounding matrix during sorption processes, while entropy signifies the degree of disorder and quality of these conversions (Goudjinou and al., 2017).

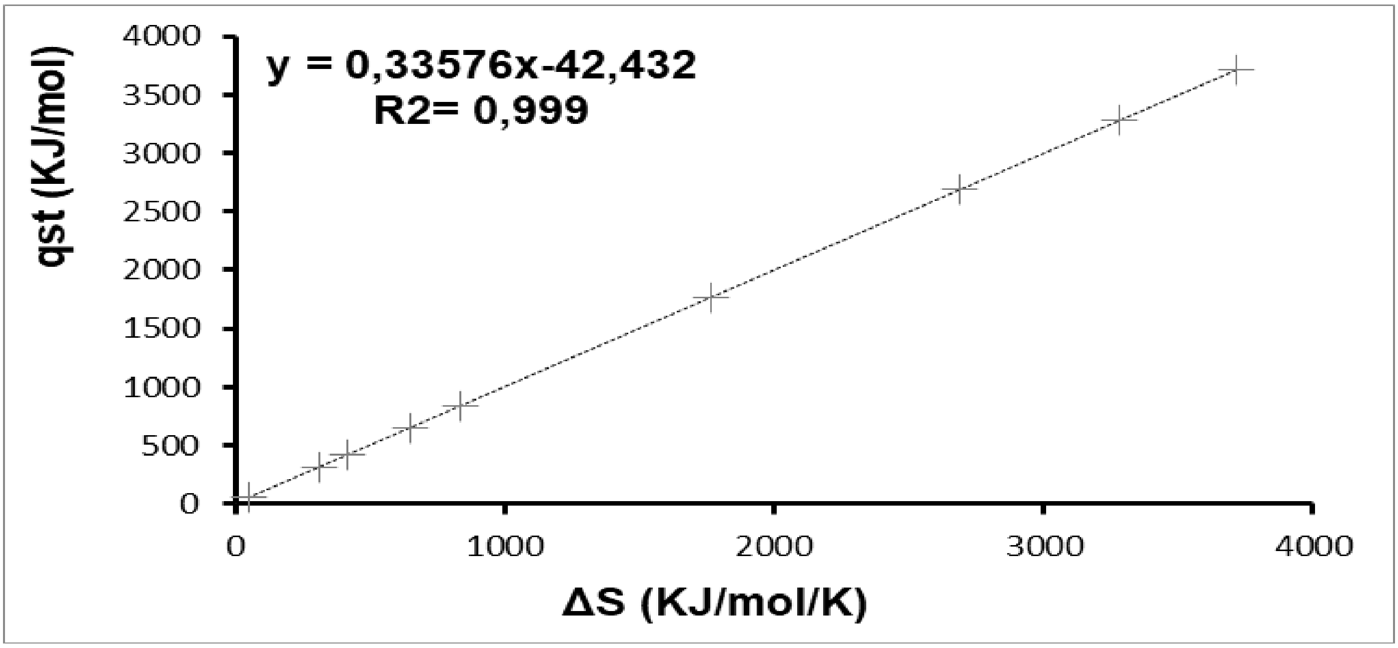

Fig 10 Enthalpy-Entropy Compensation in Peulh Cheese at Various Temperatures 30, 40, 50 and 60°C.

- *Energy of Activation*

The activation energy is defined as the amount of energy required to initiate a chemical reaction. Specifically, it represents the free enthalpy difference between the transition state and the initial state of the reaction. By applying least squares theory to linearize the curve represented by $ln(Xm) = f(1/T)$,, we were able to determine the slope, which corresponds to $\frac{-E_a}{R}$, and the y-intercept, $ln(XO)$. Consequently,the activation energy (E_a) derived from the GAB monolayer is calculated to be $-13.1009539 K/mol$, with a collision frequency (XO) of 0.45646% on a dry basis. The negative activation energy value indicates that the cheese desorption process is exothermic.

V. CONCLUSION

Determining the desorption isotherms is essential for the preservation of Peulh cheese. These isotherms, derived using the static gravimetric method, were effectively modeled with the GAB equation at temperatures of 40, 50, and 60 °C. The findings reveal that the equilibrium water content decreases as temperature increases across the entire range of water activity (from $5.5\% to 82.3\%$). The isotherms display a sigmoidal shape (type II), indicative of multimolecular adsorption. Residual curves comparing experimental data with theoretical GAB isotherms show minimal discrepancies at 50 °C. The net isosteric heat of sorption for Peulh cheese was calculated using the Clausius-Clapeyron equation. This heat increases with the level of dehydration and exhibits an exponential relationship with equilibrium water content. An empirical exponential correlation was established to describe this interaction. Furthermore, the principles of enthalpy-entropy compensation and isokinetic theory effectively elucidate the influence of temperature on the desorption process of Peulh cheese.By analyzing these thermodynamic parameters, it becomes possible to simulate optimal drying conditions for Peulh cheese, enhancing its preservation and quality.

- *Funding*

This research was not funded by any specific grants from public, commercial, or non-profit funding agencies.

- *Contributions of Authors*

GOUDJINOU Codjo wrote this paper with input from all authors, GOUDJINOU Codjo, AGUEMON Uriel and AHOUANNOU Clément. GOUDJINOU Codjo suggested the models. AGUEMON Uriel and TCHIEKRE Michel Henri Daugny performed the analytic calculations and the numerical simulations. AHOUANNOU Clément contributed to the analysis of the results.

- *Conflict of Interest Statement*

The authors declare no conflicts of interest associated with this manuscript.

REFERENCES

[1]. Stephen Campbell, Jean-philippe Chancelier, Ramine Nikoukhah, modeling and simulation in Scilab/Scicos, Springer, 2006.

[2]. SAMIR KENOUCHE, Algorithmes d'optimisation : application à des fonctions-objectifs non-linéaires, Master Physique, DÉPARTEMENT DES SCIENCES DE LA MATIÈRE-UMKB, MÉTHODES MATHÉMATIQUES ET ALGORITHMES POUR LA PHYSIQUE, 2018.

[3]. K. Madsen, H.B. Nielsen, O. Tingleff, METHODS FOR NONLINEAR LEAST SQUARES PROBLEMS, Avril 2004.

[4]. Aude Rondepierre, méthodes numériques pour l'optimisation non linéaire déterministe, Département Génie Mathématique et Modélisation, 2018.

[5]. Henri P. Gavin, The Levenberg-Marquardt algorithm for nonlinear least squares curve-fitting problems, Department of Civil and Environmental Engineering Duke University, septembre 2020.

[6]. Ananth Ranganathan, The Levenberg-Marquardt Algorithm, Juin 2004.

[7]. Marius Kaltenbach, The Levenberg-Marquardt Method and its Implementation in Python, Master Thesis, Department of Mathematics and Statistics Konstanz, Décembre, 2022.

[8]. Levenberg Kenneth, A Method for the Solution of Certain Non-Linear Problems in Least Squares, Quarterly of Applied Mathematics, 1944.

[9]. Marquardt Donald, An Algorithm for Least-Squares Estimation of Nonlinear Parameters, SIAM Journal on Applied Mathematics, 1963.

A. Ferradji, M.A.A. Matallah et A. Malek, Conservation des Dattes 'Deglet Nour' Isothermes d'adsorption à 25, 30 et 40 °C,Revue des Energies Renouvelables SMSTS'08 Alger (2008) 207-219, 2008.

[10]. Cazzaniga, A., Marcela, B.M. and Andres, L.R. (2022) Evaluation of Sorption Isotherms in Snacks with Pregelatinized Cassava. Repositorio Español de Ciencia y Tecnología, 38, 28-35. https://doi.org/10.36995/j.recyt.2022.38.004.

[11]. Ahouannou C, Jannot Y, Sanya E, Degan G (2010). Détermination expérimentale et modélisation des isothermes de désorption de produits agricoles tropicaux. Afrique Science, 06 (3) : 1-17.

[12]. Ahouannou Clément, Goudjinou Codjo, Osséni G. Sibiath, Adounkpe Julien, Hounkpatin Waliou Amoussa, Kounouhewa Basile (2023) : Estimation of Thermodynamic Parameters for Better Conservation of Fresh Tomato (Lycopersicum esculentum) ; Advances in Chemical Engineering and Science, 13, 149-171.

[13]. Aïssi VM, Soumanou MM, Bankolé H, Toukourou F, de Souza CA. 2009. Evaluation of hygienic and mycological quality of local cheese marketed in Benin. Aust. J. Basic Appl. Sci., 3(3): 2397-2404.

[14]. Allavo TUM A, Houssou PAF, Gbewadinou M E, Dansou V, Hotegni A B, Hongbété F (2023) : Stabilisation du fromage de soja (Amonsoja) à travers l'amélioration de la technologie de transformation au Bénin Revue Africaine d'Environnement et d'Agriculture; 6(4), 14-22 http://www.rafea-congo.com.

[15]. Al-Muhtaseb A H, McMinn W A M, Magee T R A (2004). Water sorption isotherms of starch powders. Part I: Mathematical description of experimental data, J Food Eng, (61): 297–307.

[16]. Benhamou A, Kouhila M, Zeghmati B, Benyoucef B (2010). Modélisation des isothermes de sorption des feuilles de marjolaine. Revue des Energies Renouvelables, 13 (2): 233-247

[17]. Benseddik A, Azzi A, Allaf K A (2014). Modélisation des isothermes de désorption de la citrouille en vue de leur séchage. Revue des Energies Renouvelables SIENR'14 Ghardaïa : 173 -182.

[18]. Bidias, J.B., Mouthe Anombogo, G.A., Ndjeumi, C.C., Djomdi, T.G.B. and Nsouandele, J.L. (2022) Study of Water Desorption Isotherms from Cocoa Beans (Theobroma Cacao L.) of Cameroon. European Scientific Journal, 18, 1. https://doi.org/10.19044/esj.2022.v18n11p Binama M P (2017). Analyse des proportions de poissons locaux et importés vendus aux marchés d'Alivia et Liberté dans la commune de Masina. Mémoire de fin d'étude présenté et défendu en vue de l'obtention du grade de Licencié en Sciences, Fac. Sciences, 60 p.

[19]. Boki K, Ohno S, Shinoda S (1990). Moisture sorption characteristics of kudzu starch and sweet potato starch, Jounal Food Sciences, 55 (1): 232-235.

[20]. BRITO Thibauthéon Arron Sonagnon, ABOUDOU Kowiou, GOUDJINOU Codjo, ALIDOU Chérif, ZANNOU Aimé, GBAGUIDI Magloire et SOUMANOU Mohamed Mansourou (2021) QUALITÉS PHYSICO-CHIMIQUE ET MICROBIOLOGIQUE DE DEUX ESPÈCES DE POISSONS IMPORTÉS (TRACHURUS TRACHURUS ET SCOMBER SCOMBRUS) ET LOCAUX (CLARIAS GARIEPRINUS ET OREOCHROMIS AUREUS) COMMERCIALISÉS AU BÉNIN Urbain ; Rev. Ivoir. Sci. Technol., 38 (2021) 311 - 323.

[21]. Brunauer S, Emmet P H, Teller E (1938). Adsorption of gases in multimolecular layers.Journal of the American Chemical Society, (60): 309-319.

[22]. Dossou J., 2004. Amélioration de la technologie traditionnelle de fabrication du fromage peulh au Bénin. Proposition de recherche DNSA/FSA/ Université d'Abomey-Calavi, 51p.

[23]. Dossou J., Adoté S. et A. Soulé., 2006. Fiche technique de production et transformation du lait frais en fromage peulh au Bénin. Département de Nutrition et Sciences Alimentaire, Faculté des Sciences Agronomiques, Université d'Abomey-Calavi, 33 pp.

[24]. Dossou Joseph Montcho Jules Karel Londji Serge Atchouké G. Donald Laurent Odjo Sylvanu (2016) Procédé Amélioré De Conservation Et De Stabilisation Du Fromage Peuhl Par L'effet Combiné Du Traitement Thermique Et Du Conditionnement Sous Vide European Scientific Journal December edition vol.12, No.36 1857- 7431 189.

[25]. Espe M, Nortvedt R, Lie Ø, Hafsteinsson H. 2002. Atlantic salmon (Salmo salar, L) as raw material for the smoking industry. II: Effect of different smoking methods on losses of nutrients and on the oxidation of lipids. Food Chem., 77 : 41– 46.

[26]. FAO (2011). Global food losses and food waste. Study conducted by J. Gustavsson, C. Cederberg, U. Sonesson for the International Congress at Interpack, Düsseldorf, Germany. Gabas AL, Telis VRN, Sobral PJA, Telis-Romero J (2007). Effect of maltodextrin and arabic gum in toilets vapor sorption thermodynamic properties of vacuum dried pineapple pulp powder. Journal of Food Engineering, 82: 246-252.

[27]. Giraldo GCE, Gloria I, Orrego-Alzate, LM, Grajales VN, Telis, AL, Gabas J, Telis R (2011). Effect of drying methods on the thermodynamic properties of blackberry pulp powder efecto del método de secado en las propiedades termodinámicas de pulpa de mora en polvo Red de Revistas Científicas de América Latina: Sistema de Información Científica, 78, (168): 139-148.

[28]. Gomaa EA, Gray JI, Rabie S, Lopez-Bote C, Booren AM. 1993. Polycyclic aromatic hydrocarbons in smoked food products and commerical liquid smoke flavourings. Food Add. Cont., 10(5): 503-521.

[29]. Goudjinou C (2018) : ''Etude théorique et expérimentale du séchage solaire des feuilles de Moringa oleifera (Lam) : Etat des lieux,caractérisation thermophysique, physico-chimique et fonctionnelle de la poudre dérivée''.thèse de docotrat université d'abomey-calavi.

[30]. Goudjinou C, Ahouannou C, Chaffa G, Soumanou MM (2017). Thermophysical characterization of the powder resulting from the solar drying of the Moringa oleifera leaves. International Journal of Engineering, Science and Technology, 9 (4): 28-47.

[31]. Goudjinou, C. (2018) Theoretical and Experimental Study of Solar Drying of Moringa oleifera Leaves (Lam.): Place of the Place, Thermophysical, Physico-Chemical and Functional Characterization of Derived Powder. Doctoral Thesis, University of Abomey Calavi, Abomey-Calavi, 175.

[32]. Goula AMG, Karapantsios TD, Achilias DS, Adamopoulos KG (2008). Toilets sorption isotherms and glass transition temperature of spray dried tomato pulp, Journal of Food Engineering, 85: 73-83.

[33]. Iglesias HA, Chirife J (1976). On the local isotherm concept and mode of moisture bindings in food products. Journal of Agriculture and Food Chemistry, 24 (77): 1342–1353.

[34]. Iglesias HA, chirife J (1982). Water sorption parameters for food and food components, Handbook of food isotherms, Academics press, New York, 37p.

[35]. Kakou KE, Akmel DC, Abouo N V, Assidjo NE, Niamké LS (2015). Isotherme d'adsorption d'eau des fèves de cacao (theobroma cacao l) Marchand. European Scientific Journal, 11 (12): 355 -370.

[36]. Kazerouni N, Sinha R, Che-Han H, Greenberg A, Rothman N. 2001. Analysis of 200 food items for benzo[a]pyrene and estimation of its intake in an epidemiologic study. Food Chem. Toxicol., 39 : 423–436.

[37]. Kèkè M, Yèhouénou B, de Souza C, Sohounhloué DCK. 2009. Evaluation of hygienic and nutritional quality of peulh cheese treated by Sorghum vulgaris (L) and Pimenta racemosa (Miller) extracts. Scientific Study, Research, 10(1) :29-46.

[38]. Kiranoudis CT, Maroulis ZB, Tsami E, Marinos-Kouris D (1993). Equilibrium moisture content and heat of desorption of some vegetables. Journal of Food Engineering, 20: 55-74.

[39]. ABOUDOU Kowiou ALIDOU, Chérif 1, VODOUHE-EGUEH2 Sènan, GOUGBE-SEMAKO Alice, SAGBOHAN Ginette Tadagbé et Mohamed SOUMANOU (2021) : Aptitude technologique de deux coagulants (Calotropaïne et Papaïne) à la production du fromage peuhl produit au Bénin Afrique SCIENCE 19(6) 122 - 132.

[40]. Krug RR, Hunter WG, Grieger RA (1976). Enthalpy-entropy compensation some fundamental statistical problems associated with the analysis of van't Hoff and Arrhenius dated. Journal of Physical and Chemistry, 80: 2335-2341.

[41]. Labuza TP, Kaane A, Chen, JY (1985). Effect of temperature on the moisture sorption isotherms and water activity shift of two dehydrated foods. Journal of Food Science, 50: 385-391.

[42]. Madamba P S, Driscoll, RH, Buckle, KA (1996). Enthalpy-entropy compensation models for sorption and Browning of garlic. Journal of Food Engineering, 28: 109-119.

[43]. MAEP, 2017. Plan Stratégique de Développement du Secteur Agricole (PSDSA) 2025 et Plan National d'Investissements Agricoles et de Sécurité Alimentaire et Nutritionnelle PNIASAN 2017 -2021, 131p.FAO, 2016.

[44]. Maroulis ZB, Kiranoudis CT and Marinos-Kouris D (1995). Heat and mass transfer modeling in air drying of foods. Journal of Food Engineering, 26 : 113–130.

[45]. Medeiros M L, Ayrosa AMIB, Pitombo RNM, Lannes SCS (2006).Sorption isotherms of cocoa and cupuassu products. Journal of Food Engineering, 73: 402-406.

[46]. Nout R, Hounhouigan DJ, van Boekel T. 2003. Les Aliments : Transformation, Conservation et Qualité. Backhuys Publishers : Leiden, Netherlands; 279p.

[47]. O. A. ALALADE and J. A. ADENEYE, The effects of storage period on the chemical composition and coliform microfloral of wara cheese. Int.J.Dairy Sci. 1(2) (2006) 126 -130.
[48]. Philippe SESSOU, Souaïbou FAROUGOU, Paulin AZOKPOTA, Issaka YOUSSAO, Boniface YEHOUENOU, Serge AHOUNOU et Dominique CODJO KOKO SOHOUNHLOUE (2013) : Inventaire et analyse des pratiques endogènes de conservation du wagashi, un fromage traditionnel produit au Bénin Int. J. Biol. Chem. Sci. 7(3): 938-952.
[49]. Salgado MC (1994). Modelling of toilets activity and enthalpy of toilets sorption in cassava chips, Drying Technology, 12: 1743-1752.
[50]. Smith SE (1947). The sorption of water vapour by high polymers, J Am Soc, 69: 646-657.
[51]. Swana W L, Mungongo PM, Nzadimwena LK, Kilingwa,C M, Mutanda, S K Kiamfu VP(2019). Proportion de vente des poissons frais locaux et importés dans les marchés de Kinshasa en République Démocratique du Congo (cas des marchés de la Liberté et Central de Kinshasa), Journal of Applied Biosciences, 141 : 14353 - 14363.
[52]. Tsami E, Maroulis Z B, Morunos-Kouris D, Saravacos, GD (1990). Heat of sorption of water in dried fruits, International Journal of Food Science Technology, 25 : pp 350-359.